ChemComm

COMMUNICATION

View Article Online
View Journal | View Issue

Cite this: *Chem. Commun.*, 2021, **57**, 1895

Received 28th October 2020,
Accepted 12th January 2021

DOI: 10.1039/d0cc07119f

rsc.li/chemcomm

A general strategy to prepare atomically dispersed biomimetic catalysts based on host–guest chemistry†

Xiao Han,‡[a] Zheng Chen,‡[bc] Wenxing Chen,‡[bd] Chunlin Lv,[e] Yongjun Ji,[fg] Jing Li,[g] Weng-Chon Cheong,[b] Xiaojuan Lei,[a] Qing Peng,[b] Chen Chen,[b] Dingsheng Wang,[b] Chao Lian*[hd] and Yadong Li[b]

Herein, we report a general strategy based on host–guest interactions to fabricate atomically dispersed biomimetic catalysts, which were evaluated by diboration of phenylacetylene. The structure and function of these mimics are quite similar to those of enzymes, namely, the atomically dispersed metal serves as an active site, the external macromolecular structure plays a role as an enzyme catalytic pocket to stabilize the reaction intermediates and the interactions between the intermediates and functional groups near to the active site can reduce the reaction activation energy.

Enzymes, natural biocatalysts that catalyze all reactions to support biological life, exhibit outstanding activity and selectivity under mild conditions, and are generally much more efficient than traditional chemical catalysts.[1] It is generally recognized that the superior catalytic properties of enzymes often emanate from the substrate–enzyme complex's molecular binding and chemical transformations, facilitating the formation of stabilized transition states, mediated by non-covalent interactions involving van der Waals and π–π interactions, hydrophilic/hydrophobic effects and electrostatic interactions.[2] This has inspired the rise of supramolecular or host–guest catalysis, which involves the preparation of biomimetic catalysts mimicking enzymes based on various host–guest interactions from the distinct chemical environments inside and outside the cavities of host molecules,[3] such as cyclodextrins,[4] calixarenes,[5] cucurbiturils,[6] hemicryptophanes[7] or other artificial synthetic hosts.[8] However, the design and fabrication of these supramolecular mimics still relies on modulation of the chemical environment around the catalytic active sites. It is certainly a giant leap for synthesis and catalysis to directly build up enzyme mimic structures based on easy-to-control heterogeneous catalyst supports with mimicked enzyme catalytic pockets.

In recent decades, atomically dispersed metal catalysts, so-called single-atom catalysts, have attracted increasing research attention.[9–11] In these novel heterogeneous catalysts, uniform single atoms act as isolated active sites, which builds a bridge between heterogeneous and homogeneous catalysis by supplying insight into the catalysis process at the molecular level.[12–16] From a structural aspect, these single atom sites most look like the simplest active sites in enzymes. Because transition metals in a single-atom state can easily aggregate into nanoparticles, several restriction factors, such as metal–support interactions,[9,13,17] coordination interactions,[11,18] steric confinements[19] and defect effects,[15,20–22] are utilized to stabilize single-atom metal atoms on the support during the fabrication of atomically dispersed metal catalysts. With regard to enzyme mimics, in addition, host–guest interactions between the substrate and mimics are promising to stabilize single-atom metal atoms as well.

Base on host–guest chemistry, we propose a general strategy to prepare atomically dispersed biomimetic catalysts, where the catalytic sites are located in the host units that mimic enzyme catalytic pockets on the supports (Fig. 1a). In this strategy, hydrophobic transition metal precursors are incorporated into the cavities of the host units. The metal atoms in the formed inclusion complexes are further reduced to generate single catalytic sites located in the cavities mimicking enzyme

[a] *Department of Chemistry, School of Science, Beijing Jiaotong University, Beijing, 100044, P. R. China*
[b] *Department of Chemistry, Tsinghua University, Beijing 100084, China*
[c] *Key Laboratory of Functional Molecular Solids, Ministry of Education, Anhui Key Laboratory of Molecule-Based Materials, College of Chemistry and Materials Science, Anhui Normal University, Wuhu 241000, P. R. China*
[d] *Beijing Key Laboratory of Construction Tailorable Advanced Functional Materials and Green Applications, School of Materials Science and Engineering, Beijing Institute of Technology, Beijing 100081, P. R. China*
[e] *School of Pharmacy and Center on Translational Neuroscience, Minzu University of China, Beijing 100081, P. R. China*
[f] *School of Light Industry, Beijing Technology and Business University, Beijing 100048, P. R. China*
[g] *State Key Laboratory of Multiphase Complex Systems, Institute of Process Engineering, Chinese Academy of Sciences, Beijing, 100190, P. R. China*
[h] *Beijing Single-atom Site Catalysis Technology Co., Ltd, Beijing 100094, P. R. China. E-mail: lianchao@sacatalysis.com*

† Electronic supplementary information (ESI) available: Experimental procedure, additional data, *etc.* See DOI: 10.1039/d0cc07119f

‡ These authors contributed equally.

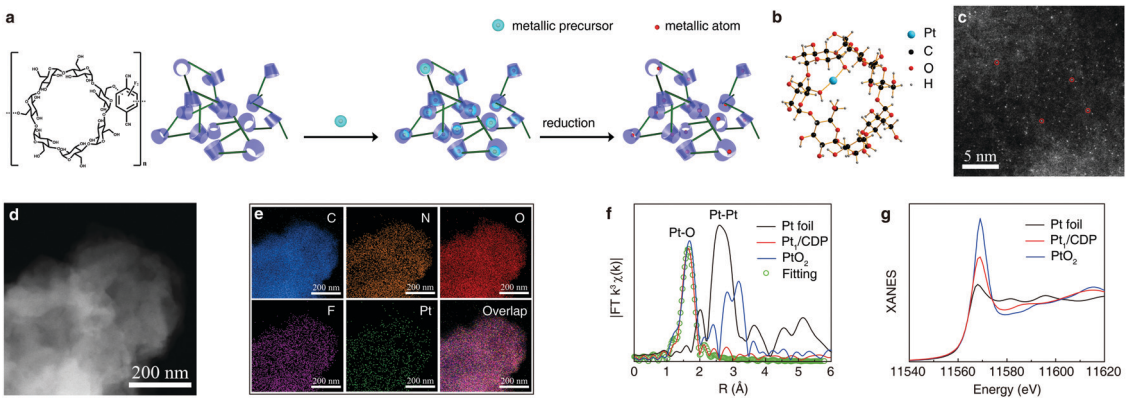

Fig. 1 (a) Schematic illustration of the synthesis of the atomically dispersed biomimetic catalysts in this work. (b) Schematic model of the mimicked enzyme catalytic pocket in Pt_1/CDP. (c) Aberration-corrected high-angle annular dark-field scanning transmission electron microscope (HAADF-STEM) image of Pt_1/CDP. (d) HAADF-STEM image of Pt_1/CDP. (e) Corresponding element (C, N, O, F and Pt) maps of Pt_1/CDP. (f) Fourier-transformed EXAFS spectra at the Pt L_3-edge for Pt_1/CDP, Pt foil and PtO_2, and the EXAFS fitting curve for Pt_1/CDP. (g) The normalized XANES spectra at the Pt L_3-edge for Pt_1/CDP, PtO_2 and Pt foil.

catalytic pockets. To confirm the feasibility of this strategy, a reported β-cyclodextrin (CD)-containing polymer (CDP) was used as a support to synthesize a series of atomically dispersed biomimetic catalysts (M_1/CDP, M = Pt, Co, Ni, Cu, Ru, Rh and Ir). It was proved that this enzyme mimic structure exhibits a catalytic activity enhancement with diboration of alkynes over platinum catalysts as a model reaction.

The CDP support was synthesized *via* an established method,[23] with some modifications (Fig. S1 and S2, ESI†). Taking Pt_1/CDP as an example, bis(2,4-pentanedionate) platinum(II) ($Pt(acac)_2$, used as a Pt precursor) and the support were stirred in water for one day to form an inclusion complex of CDP with $Pt(acac)_2$. For the inclusion, $Pt(acac)_2$ was encapsulated into the host units (β-CD in the framework of CDP) at a molecular level so that no XRD signal for the $Pt(acac)_2$ crystals can be observed (Fig. S3, ESI†). Finally, the Pt_1/CDP product was obtained by reducing the included $Pt(acac)_2$ molecules with $NaBH_4$. As shown in Fig. 1c and d, platinum was in an atomically dispersed state, in which no Pt nanoparticles could be observed, throughout the as-synthesized Pt_1/CDP composite. EDX analysis in STEM revealed that this atomic Pt was dispersed in the CDP support evenly (Fig. 1e). The Pt content of the final sample was 0.8%, according to ICP-AES analysis (Table S2, ESI†), which was in accordance with the target Pt loading in the synthesis stage. EXAFS and XANES were used to further verify the atomically dispersed nature of Pt_1/CDP (Fig. 1f, g and Fig. S4, S5, Table S3, ESI†). As shown in Fig. 1f, a notable single peak in the region of 1 to 2 Å can be assigned to Pt–O bonds, but no signal in the region of 2 to 3 Å from the Pt–Pt contribution was observed. In comparison with Pt foil, an enhanced white-line intensity of Pt_1/CDP with a small shift to higher energy for the absorption edge suggested that partially oxidized $Pt^{\delta+}$ rather than Pt^0 existed in Pt_1/CDP (Fig. 1g). This agreed well with the result of XPS measurement, in which the binding energy of the Pt $4f_{7/2}$ core-level in Pt_1/CDP was obviously higher than that for traditional zero-valent metallic Pt (Table S4, ESI†). Because the strategy proposed in this work resorts to the general host–guest interactions that are mainly influenced by the relative size of the cavity in the host units and the hydrophobic guest precursor molecules, this synthesis method is effective for a variety of atomically dispersed transition metal catalysts. By means of using appropriate transition metal complexes as precursors, the inclusion between CDP and the precursors could be achieved as well (Fig. S6, ESI†), and the corresponding atomically dispersed transition metal catalysts, such as Co_1/CDP, Ni_1/CDP, Cu_1/CDP, Ru_1/CDP, Rh_1/CDP and Ir_1/CDP, would be obtained by reducing the transition metal complex encapsulated in CDP (Fig. S8–S14 and Tables S3, S4, ESI†). Lots of nanoparticles appeared, however, when a transition metal complex, tris(2,4-pentanedionate) ruthenium(III) for example, which is larger than the CD cavity was used as a precursor (Fig. S15, ESI†). This further implied the host–guest chemistry interaction involved in this strategy.

To verify the catalytic performance of this enzyme-like structure, Pt-catalyzed diboration of phenylacetylene (**1a**) with bis(pinacolato)diboron (B_2pin_2, **2a**) was chosen as a model reaction (Table 1). Pt_1/CDP exhibited a higher catalytic activity compared with the reported heterogeneous catalysts under similar reaction conditions.[23] The reaction conditions were optimized and the best test conditions were that the diboration reaction was carried out in toluene at 100 °C (Table 1, entry 1–7). By virtue of the enzyme-like structure, the activity of Pt_1/CDP (898 h^{-1}, Table 1, entry 6) was almost 13.5 times higher than that of Pt_1/CN (62 h^{-1}, Table 1, entry 8), an atomically dispersed platinum catalyst without this specific structure (Fig. S16, ESI†). It was found that the atomically dispersed state for the single-atom Pt catalyst did not favor the catalytic diboration reaction because the Pt nanocrystals, with an average diameter of 2 nm, adsorbed on the active carbon (Fig. S17 and S18, ESI†) exhibited a higher catalytic activity (176 h^{-1}, Table 1, entry 9) compared with Pt_1/CN. Moreover, when we adsorbed the Pt nanocrystals on CDP (Fig. S19, ESI†), a slight decrease in catalytic activity was observed (160 h^{-1}, Table 1, entry 10). It has been reported that the CDP used in this work is a

Table 1 Pt-Catalyzed diboration of phenylacetylene.[a]

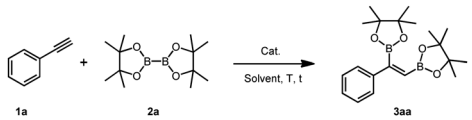

Entry	Catalyst	Sol.	Temp. (°C)	T (h)	Con.[b] (%)	Sel.[b] (%)	TOF (h^{-1})
1	Pt_1/CDP	DMF	60	1	3.2	91.2	32
2	Pt_1/CDP	1,4-Dioxane	60	1	10.3	100	103
3	Pt_1/CDP	MeCN	60	1	4.1	98.9	41
4	Pt_1/CDP	Toluene	60	1	30.9	100	309
5	Pt_1/CDP	Toluene	80	1	79.3	100	793
6	Pt_1/CDP	Toluene	100	1	89.8	100	898
7	Pt_1/CDP	Toluene	100	2	>99.9	100	—
8	Pt_1/CN	Toluene	100	2	12.3	100	62
9	Pt_{nano}/C	Toluene	100	2	35.2	100	176
10	Pt_{nano}/CDP	Toluene	100	2	31.9	100	160

[a] Reaction conditions: phenylacetylene (0.5 mmol), B_2pin_2 (0.55 mmol), catalyst (0.1 mmol% based on metal), solvent (2 mL). [b] Conversion and selectivity is determined by GC and GC-MS.

porous polymer,[24] and the porous structure will affect the diffusion of the reactants to bring about a decrease in apparent activity. However, it is interesting that the activity of Pt_1/CDP was also much higher than that of Pt_{nano}/CDP. Because the Pt nanocrystals were too large to enter into the β-CD cavities, these results implied that the mimicked enzyme catalytic pockets merely made a contribution to the catalytic reaction on the sites inside them to extremely improve the catalytic activity, just like what happens in enzyme catalysis. For this model reaction, the improvement of activity in the enzyme-like structure even offset the inferior activity over single-atom sites in Pt_1/CDP compared with that over multi-atom sites in nanoparticles.

We simplified the mimicked enzyme catalytic pocket structure of Pt_1/CDP into a single β-CD structure (Pt_1/CD) so that DFT calculations could be performed to further reveal the effect of the mimicked structure (Fig. S20–S24 and Videos S1–S3, ESI†). It has been reported that diboration of alkynes involves three steps, namely (I) oxidative addition of a B–B bond to the Pt site, (II) insertion of a C–C multiple bond and (III) reductive elimination of the C–B bond from the Pt site.[21] As shown in Fig. 2, step III, with an energy barrier (20.1 kcal mol^{-1}) slightly higher than that of step II (19.6 kcal mol^{-1}) and much higher than that of step I (7.3 kcal mol^{-1}), is the rate-determining step over Pt_1/CD. When the cyclic structure was broken and only the molecular structure near to the Pt single-atom site remained (Pt_1/CD-b), the highest reaction energy barrier of step III was slightly reduced to 17.9 kcal mol^{-1}, but all of the related Gibbs free energies of the intermediates were elevated. This suggested that the cyclic structure of β-CD can stabilize intermediates involved in the catalytic reaction, while it cannot reduce the activation energy of the reaction. For most of the reaction intermediates in reactions over both Pt_1/CD and Pt_1/CD-b, however, it was found that there are hydrogen bonds between O in B_2pin_2 and H in hydroxyls near to the Pt single-atom site (Fig. S23 and S24, Videos S1 and S2, ESI†). The hydrogen bonding may directly affect the reaction behavior of the intermediates over the Pt sites. According to our DFT calculations, the highest energy barrier (step III) of the whole reaction process sharply elevated to 26.7 kcal mol^{-1}, once the H of hydroxyls in Pt_1/CD-b was absent (Pt_1/CD-*b*-noH). The participation of hydroxyls near to the Pt site played an important role in reducing the reaction activation energy. From the viewpoint of structure and function, the atomically dispersed biomimetic catalysts are extremely similar to enzymes, in which an external macrocyclic structure supplies an enzyme catalytic pocket to stabilize the reaction intermediates, but the interactions between the intermediates and functional groups, such as amino, carboxyl and hydroxyl in enzymes, near to the active sites contribute to reducing the activation energy.

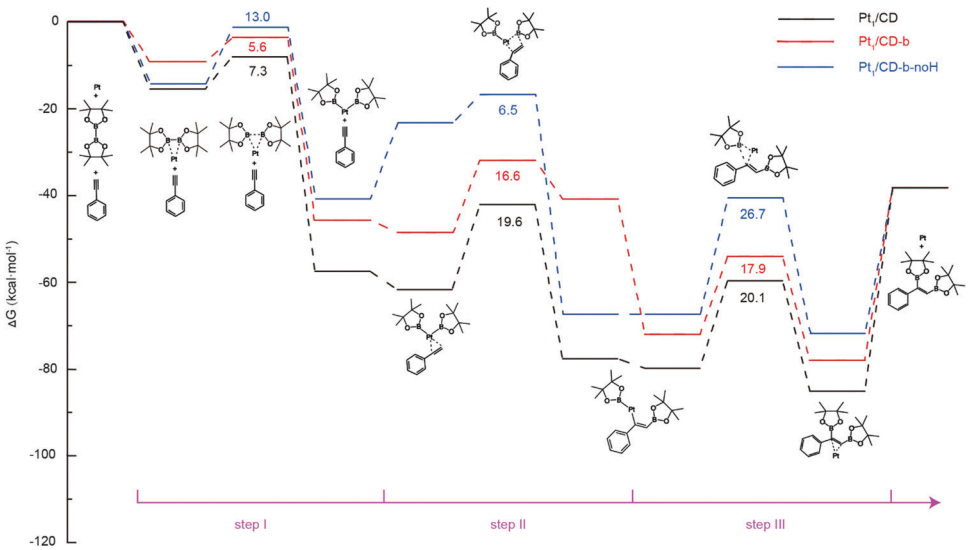

Fig. 2 Gibbs free energy profiles for the Pt-catalyzed diboration of phenylacetylene.

As shown in Fig. S25 (ESI†), the Pt_1/CDP catalyst showed a good universal significance for the catalytic diboration of alkynes. For the reaction of various substrates, diborylated products were obtained as the only products, with no by-products being detected, under the optimized reaction conditions. In addition to the 93% isolated yield of **3aa** obtained for the diboration of phenylacetylene (**1a**) with B_2pin_2 (**2a**), diboration with other boronate esters, bis(neopentylglycolate)diboron (B_2neop_2) (**2b**) for example, also worked well to provide the product **3ab** with a 91% isolated yield after a 3 h reaction under the same conditions. A difference in the substituent position in the aryl alkyne substrates exerted no influence on the catalytic efficiency of Pt_1/CDP, where *p*-ethynyltoluene (**1b**), *m*-ethynyltoluene (**1c**) and *o*-ethynyltoluene (**1d**) are diborylated to **3ba**, **3ca** and **3da** with isolated yields of 93, 91 and 92%, respectively. Furthermore, aryl alkynes with distinct substituent types can react without obvious differences in yield, while the aryl alkynes bearing electron-withdrawing groups (–Cl, –Br and $–NO_2$) need longer time to attain high yields compared with those substituted with electron-donating groups (–Me and –OMe). The reaction rate decreased with a decline in the electron-withdrawing ability of the substituents. Besides aryl alkynes, the Pt_1/CDP catalyst was also tolerant of aliphatic alkynes like cyclohexylacetylene (**1i**), and the reaction proceeded smoothly to afford the desired products with an isolated yield of 91% in 5 h.

The Pt_1/CDP catalyst exhibited excellent stability under the test conditions, which can be recovered and reused four times without any loss of catalytic efficiency (Table S5, ESI†). After the catalytic test, the structure of Pt_1/CDP was still well maintained (Fig. S26, ESI†). This further confirmed the practicability of this kind of heterogeneous biomimetic catalyst.

In summary, a general strategy based on host–guest interactions was proposed to fabricate atomically dispersed biomimetic catalysts using the macrocyclic structure in cyclodextrins. These mimics have a similar structure and function to enzymes, where the atomically dispersed metal plays a role as an active site, the external macromolecular structure serves as an enzyme catalytic pocket to stabilize the reaction intermediates and the interactions between the intermediates and functional groups near to the active site can reduce the reaction activation energy.

This work was supported by the National Natural Science Foundation of China (21701007, 21801015). We thank the XAFS station (BL14W1) of the Shanghai Synchrotron Radiation Facility and the XAFS station (1W1B) of Beijing Synchrotron Radiation Facility (BSRF). The authors sincerely thank Dr Tian Lu of Beijing Kein Research Center for Natural Sciences for his help with the DFT calculations.

Conflicts of interest

There are no conflicts to declare.

Notes and references

1 R. A. van Santen, P. W. N. M. van Leeuwen and J. A. Moulijn in *Catalysis: an Integrated Approach*, ed. B. A. Averill, Elsevier, Amsterdam, 2000; T. H. Kim, P. Mehrabi, Z. Ren, A. Sljoka, C. Ing, A. Bezginov, L. Ye, R. Pomès, R. S. Prosser and E. F. Pai, *Science*, 2017, **355**, eaag2355.
2 C. Deraedt and D. Astruc, *Coord. Chem. Rev.*, 2016, **324**, 106–122; T. Saleh and C. G. Kalodimos, *Science*, 2017, **355**, 247–248.
3 M. Raynal, P. Ballester, A. Vidal-Ferran and P. W. N. M. van Leeuwen, *Chem. Soc. Rev.*, 2014, **43**, 1660–1733; R. Villalonga, R. Cao and A. Fragoso, *Chem. Rev.*, 2007, **107**, 3088–3116.
4 R. Breslow and L. E. Overman, *J. Am. Chem. Soc.*, 1970, **92**, 1075–1077; R. Breslow and S. D. Dong, *Chem. Rev.*, 1998, **98**, 1997–2011.
5 D. M. Homden and C. Redshaw, *Chem. Rev.*, 2008, **108**, 5086–5130.
6 X. Ni, X. Xiao, H. Cong, Q. Zhu, S. Xue and Z. Tao, *Acc. Chem. Res.*, 2014, **47**, 1386–1395.
7 D. Zhang, A. Martinez and J. P. Dutasta, *Chem. Rev.*, 2017, **117**, 4900–4942.
8 M. D. Pluth, R. G. Bergman and K. N. Raymond, *Science*, 2007, 85–88; M. D. Pluth, R. G. Bergman and K. N. Raymond, *Acc. Chem. Res.*, 2009, **42**, 1650–1659; S. Das, G. W. Brudvig and R. H. Crabtree, *Chem. Commun.*, 2008, 413–424.
9 B. Qiao, A. Wang, X. Yang, L. F. Allard, Z. Jiang, Y. Cui, J. Liu, J. Li and T. Zhang, *Nat. Chem.*, 2011, **3**, 634–641.
10 X. Yang, A. Wang, B. Qiao, J. Li, J. Liu and T. Zhang, *Acc. Chem. Res.*, 2013, **46**, 1740–1748; K. Ding, A. Gulec, A. M. Johnson, N. M. Schweitzer, G. D. Stucky, L. D. Marks and P. C. Stair, *Science*, 2015, **350**, 189–192.
11 Z. Zhuang, Q. Kang, D. Wang and Y. Li, *Nano Res.*, 2020, **13**, 1856–1866.
12 Y. Zhai, D. Pierre, R. Si, W. Deng, P. Ferrin, A. U. Nilekar, G. Peng, J. A. Herron, D. C. Bell, H. Saltsburg, M. Mavrikakis and M. Flytzani-Stephanopoulos, *Science*, 2010, **329**, 1633–1636.
13 G. Kyriakou, M. B. Boucher, A. D. Jewell, E. A. Lewis, T. J. Lawton, A. E. Baber, H. L. Tierney, M. Flytzani-Stephanopoulos and E. C. H. Sykes, *Science*, 2012, **335**, 1209–1212.
14 E. C. Tyo and S. Vajda, *Nat. Nanotechnol.*, 2015, **10**, 577–588.
15 P. Liu, Y. Zhao, R. Qin, S. Mo, G. Chen, L. Gu, D. M. Chevrier, P. Zhang, Q. Guo, D. Zang, B. Wu, G. Fu and N. Zheng, *Science*, 2016, **352**, 797–801.
16 C. Zhu, S. Fu, Q. Shi, D. Du and Y. Lin, *Angew. Chem., Int. Ed.*, 2017, **56**, 13944–13960.
17 P. Hu, Z. Huang, Z. Amghouz, M. Makkee, F. Xu, F. Kapteijn, A. Dikhtiarenko, Y. Chen, X. Gu and X. Tang, *Angew. Chem., Int. Ed.*, 2014, **53**, 3418–3421; J. Jones, H. Xiong, A. T. DeLaRiva, E. J. Peterson, H. Pham, S. R. Challa, G. Qi, S. Oh, M. H. Wiebenga, X. I. P. Hernández, Y. Wang and A. K. Datye, *Science*, 2016, **353**, 150–154.
18 H. Su, P. Gao, M. Wang, G. Zhai, J. Zhang, T. Zhao, J. Su, X. Li, M. Antonietti and J. Chen, *Angew. Chem., Int. Ed.*, 2018, **57**, 15194–15198; R. Zhao, Z. Liang, S. Gao, C. Yang, B. Zhu, J. Zhao, C. Qu, R. Zou and Q. Xu, *Angew. Chem., Int. Ed.*, 2019, **58**, 1975–1979.
19 L. Liu, M. Lopez-Haro, C. W. Lopes, C. Li, P. Concepcion, L. Simonelli, J. J. Calvino and A. Corma, *Nat. Mater.*, 2019, **18**, 866–873.
20 J. H. Kwak, J. Hu, D. Mei, C. Yi, D. H. Kim, C. H. F. Peden, L. F. Allard and J. Szanyi, *Science*, 2009, **325**, 1670–1673.
21 J. Zhang, X. Wu, W. Cheong, W. Chen, R. Lin, J. Li, L. Zheng, W. Yan, L. Gu, C. Chen, Q. Peng, D. Wang and Y. Li, *Nat. Commun.*, 2018, **9**, 1002.
22 J. Wan, W. Chen, C. Jia, L. Zheng, J. Dong, X. Zheng, Y. Wang, W. Yan, C. Chen, Q. Peng, D. Wang and Y. Li, *Adv. Mater.*, 2018, **30**, 1705369.
23 Q. Chen, J. Zhao, Y. Ishikawa, N. Asao, Y. Yamamoto and T. Jin, *Org. Lett.*, 2013, **15**, 5766–5769; F. Alonso, Y. Moglie, L. Pastor-Pérez and A. Sepúlveda-Escribano, *ChemCatChem*, 2014, **6**, 857–865.
24 A. Alsbaiee, B. J. Smith, L. Xiao, Y. Ling, D. E. Helbling and W. R. Dichtel, *Nature*, 2016, **529**, 190–U146.

